4-(2'-Pyridyl)imidazole as an artificial nucleobase in highly stabilizing Ag(I)-mediated base pairs

Kristina Schweizer, Jutta Kösters, Jens Müller✉

Westfälische Wilhelms-Universität Münster

Institut für Anorganische und Analytische Chemie

Corrensstr. 28/30

48149 Münster

Germany

E-Mail: mueller.j@uni-muenster.de

Fax: +49 251 8336007

Supplementary Material

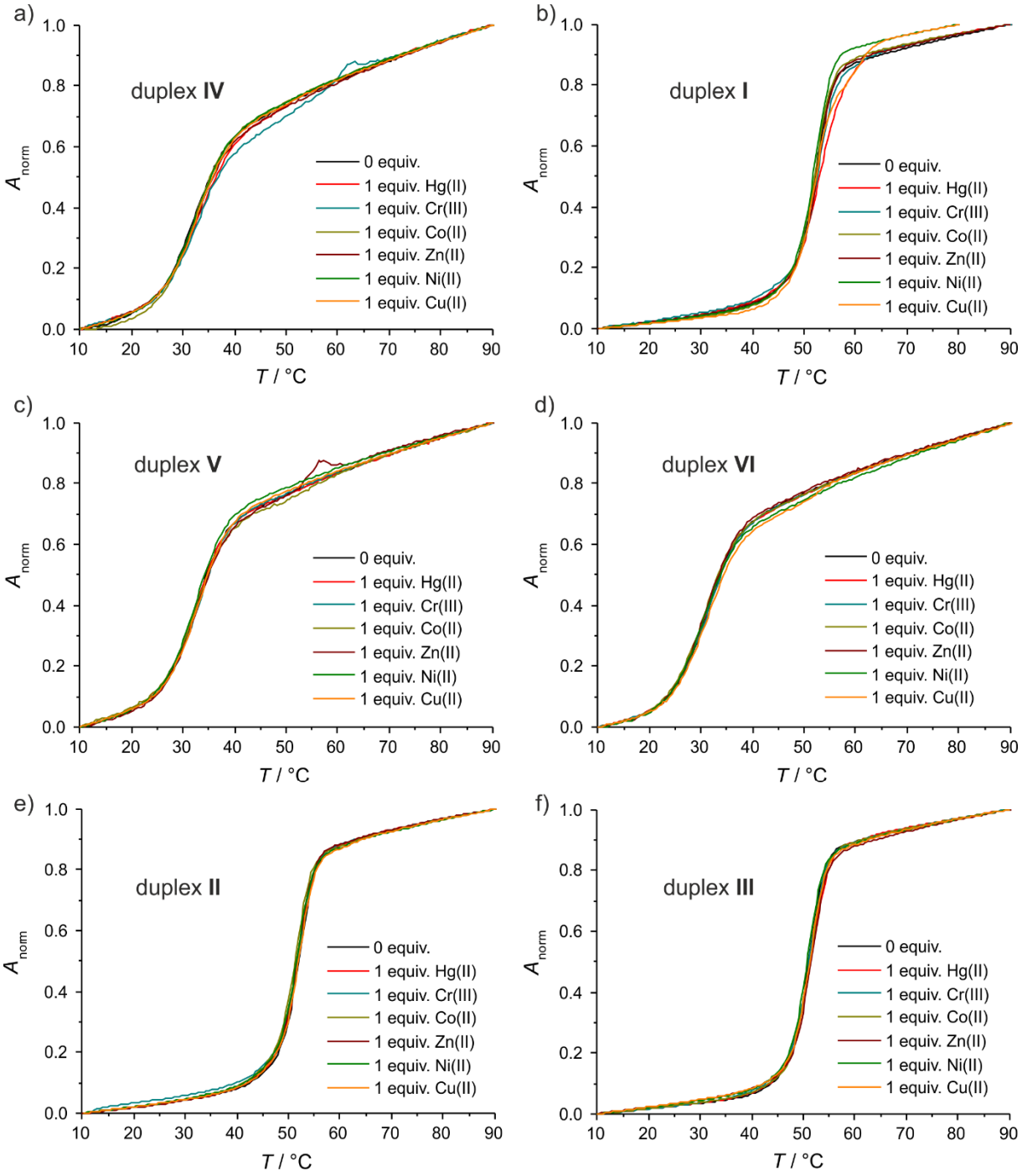

Fig. S1 Melting curves of duplexes **I** – **VI** in the absence of any transition metal salt and in the presence of one equivalent of $HgCl_2$, $Cr(NO_3)_3 \cdot 9\ H_2O$, $Co(NO_3)_2 \cdot 6\ H_2O$, $Zn(NO_3)_2 \cdot 6\ H_2O$, $Ni(NO_3)_2 \cdot 6\ H_2O$, or $Cu(NO_3)_2 \cdot 3\ H_2O$, respectively.

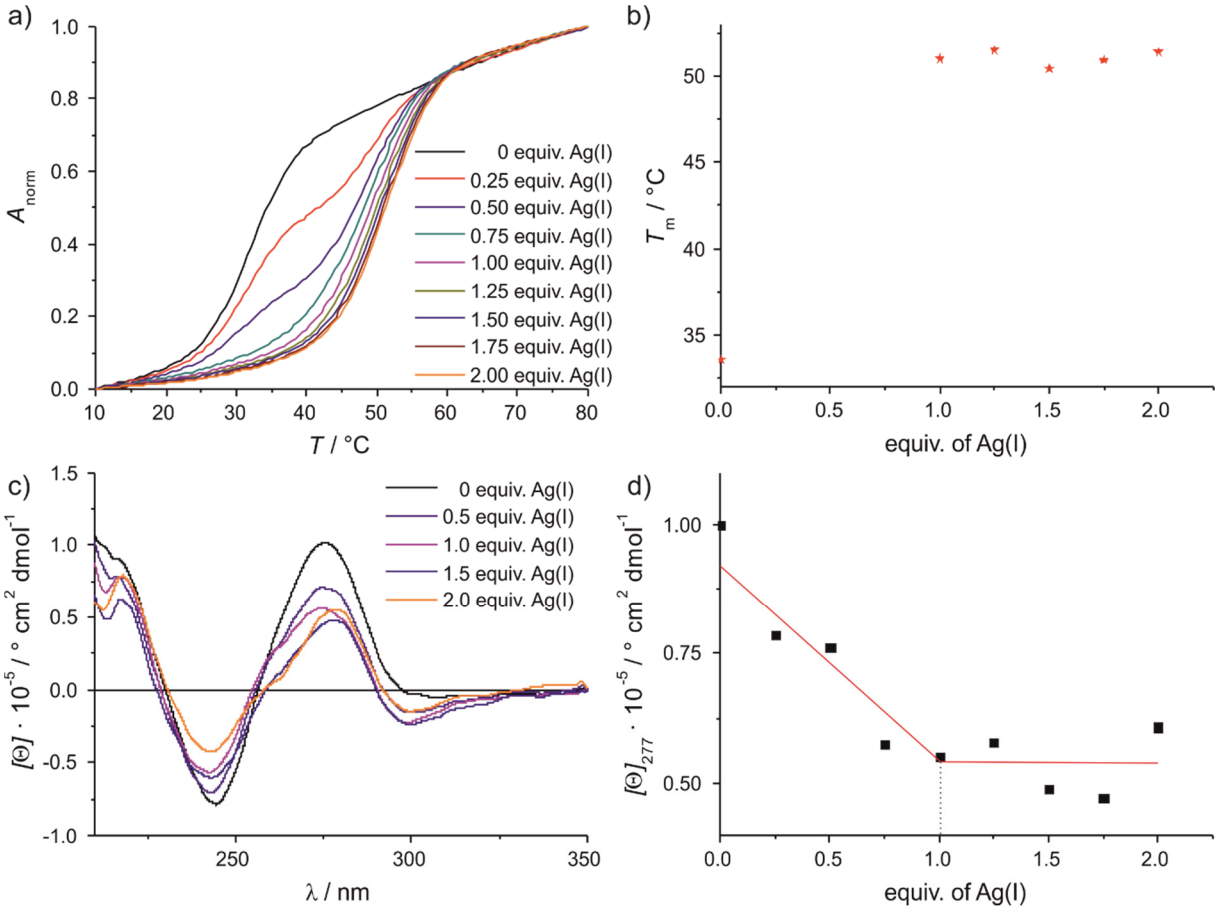

Fig. S2 Characterization of the **2**–Ag(I)–**2** base pair in duplex **IV**. a) Normalized temperature-dependent UV absorbance at 260 nm of duplex **IV** in the presence of increasing amounts of $AgNO_3$; b) plot of the melting temperature T_m of duplex **IV** versus the equivalents of Ag(I); c) CD spectra of duplex **IV** in the presence of increasing amounts of $AgNO_3$; d) plot of the molar ellipticity at 277 nm versus the equivalents of Ag(I).

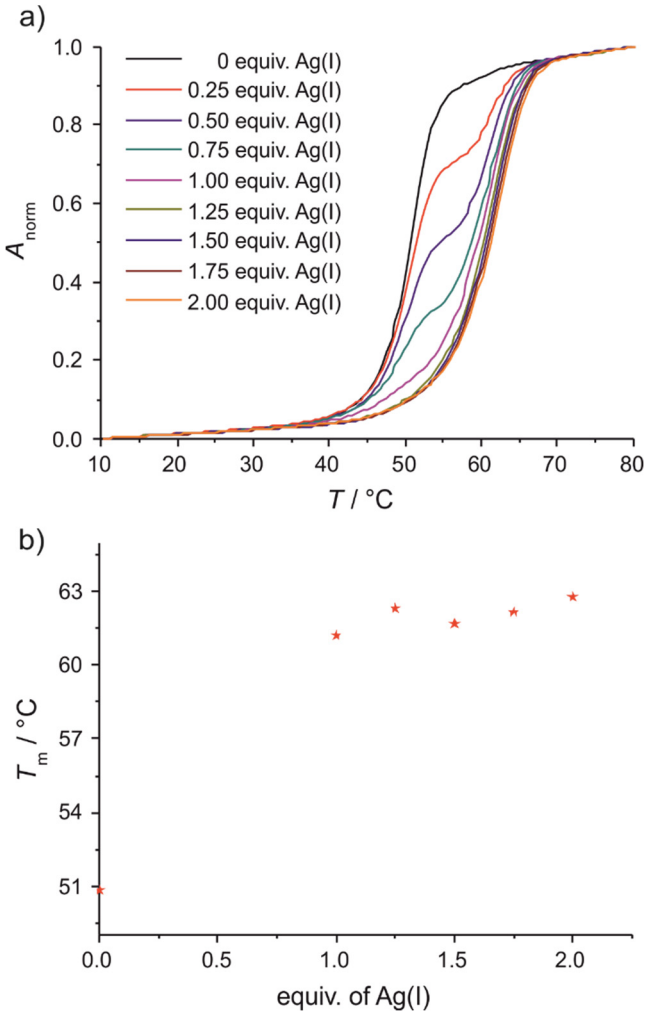

Fig. S3 Characterization of the **1**–Ag(I)–**2** base pair in duplex **III**. a) Normalized temperature-dependent UV absorbance at 260 nm of duplex **III** in the presence of increasing amounts of $AgNO_3$; b) plot of the melting temperature T_m of duplex **III** versus the equivalents of Ag(I).

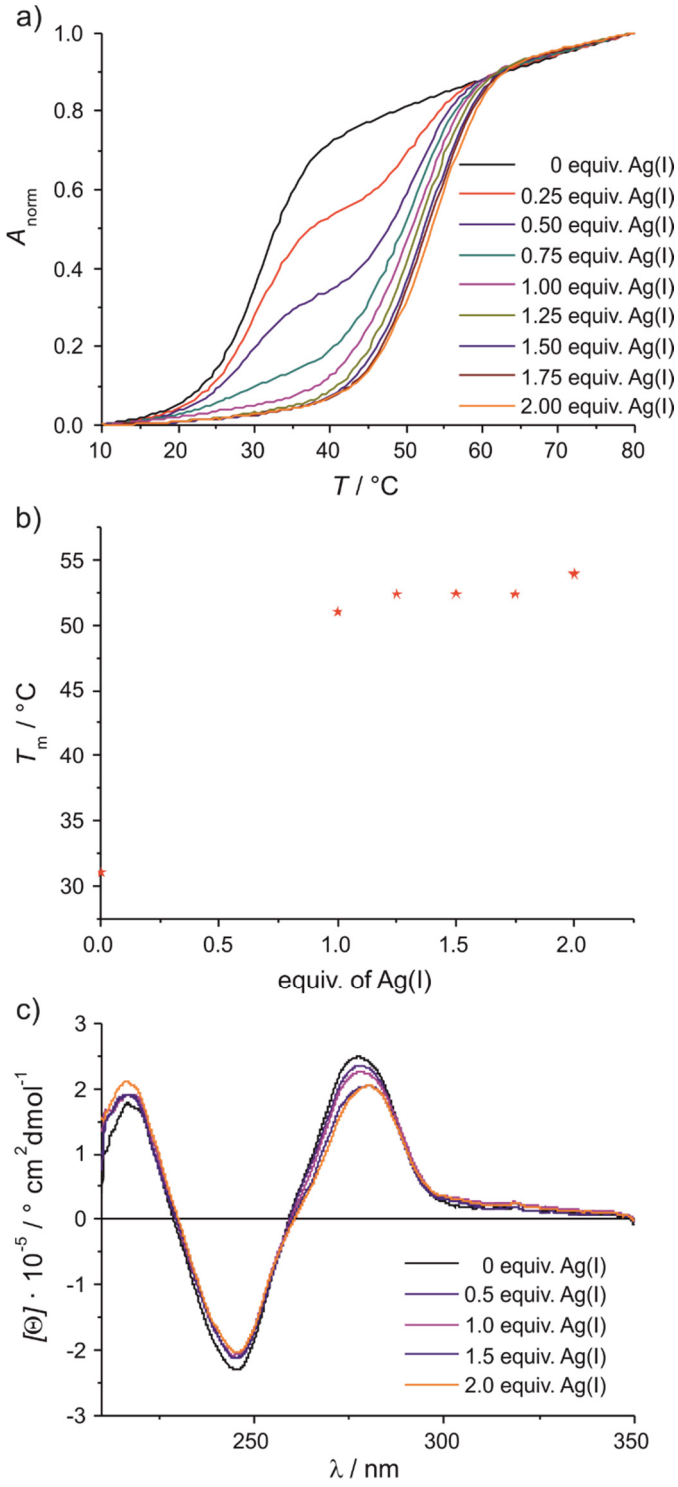

Fig. S4 Characterization of the **1**–Ag(I)–**2** base pair in duplex **VI**. a) Normalized temperature-dependent UV absorbance at 260 nm of duplex **VI** in the presence of increasing amounts of $AgNO_3$; b) plot of the melting temperature T_m of duplex **VI** versus the equivalents of Ag(I); c) CD spectra of duplex **VI** in the presence of increasing amounts of $AgNO_3$.

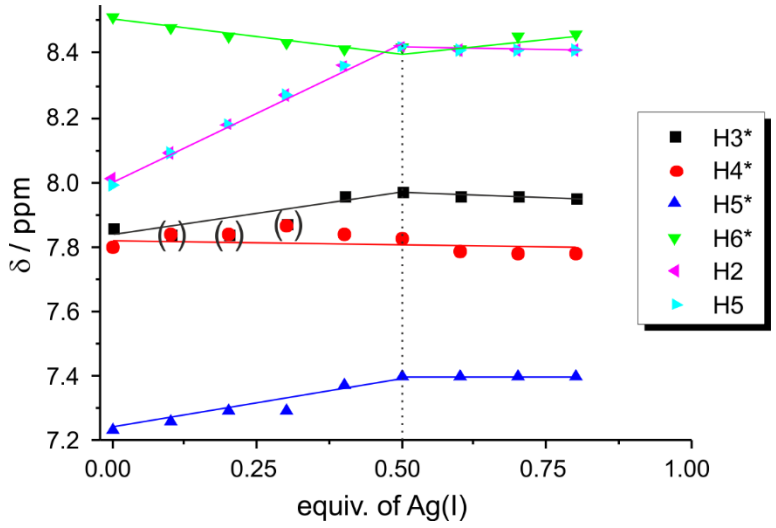

Fig. S5 Plot of the ^{1}H NMR chemical shifts of toluoyl-protected nucleoside **3** in DMSO-d_6 upon the addition of increasing amounts of $AgClO_4$. With the exception of the pyridyl H4* resonance (see Fig. 2 for the atom numbering scheme), all resonances shift significantly upon binding of **3** to Ag(I), indicating that the imidazole moiety and the pyridyl moiety are both involved in coordination to Ag(I). Due to signal overlap, the chemical shifts of the resonances of H3* and H4* in the presence of 0.1 – 0.3 equiv. of $AgClO_4$ cannot be determined unambiguously, hence the respective data points are represented in brackets.

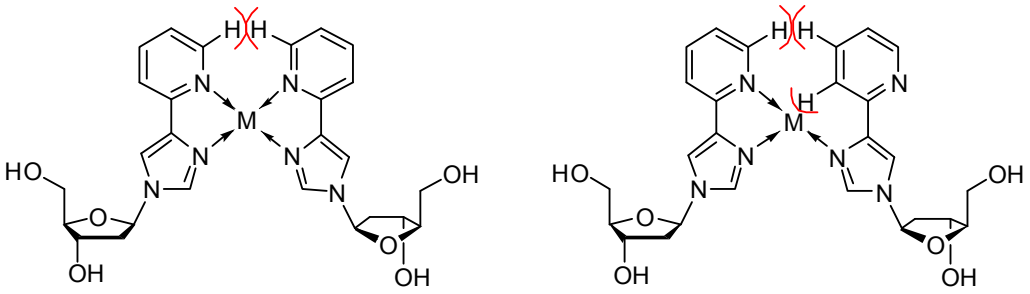

Scheme S1 Chemical structures of the **2**–Ag(I)–**2** base pair assuming a [2+2] coordination environment (left) and a hypothetical [2+1] coordination environment (right). Steric clashes in hypothetical planar structures are indicated, which would result in the formation of non-planar structures.

Table S1 Endocyclic torsion angles ν_i of the deoxyribose ring [1] that were used to calculate the phase angle of pseudorotation P [2] and the puckering amplitude ψ_m [2], the backbone torsion angle γ (O5'-C5'-C4'-C3'), and the glycosidic bond angle χ.

ν_0 / °	–19.75(2)
ν_1 / °	35.04(2)
ν_2 / °	–36.22(2)
ν_3 / °	25.92(2)
ν_4 / °	–4.11(2)
ψ_m / °	37.1(3)
P / °	167.5(3), C2'-*endo* (^2E)
χ / °	–102.9(2), *anti* (–*ac*)
γ / °	51.6(2), +*sc*

References

[1] IUPAC-IUB Joint Commission on Biochemical Nomenclature (1983) Eur J Biochem 131: 9-15

[2] Altona C, Sundaralingam M (1972) J Am Chem Soc 94: 8205-8212